

# **MCNP Analysis of a Novel W-181 HDR Brachytherapy Source**

**Submitted by Kyle Marquez**  
Advised by David Medich Ph. D.



Department of Physics, Worcester Polytechnic Institute  
April 27, 2023

This report represents the work of one or more WPI undergraduate students submitted to the faculty as evidence of completion of a degree requirements. WPI routinely publishes these reports on the web without editorial or peer review.

## **Abstract**

The aim of this paper is to evaluate the viability of tungsten-181 by comparing its dosimetric distributions directly to iridium-192, regarded as the current gold standard of brachytherapy. The radial dose function of tungsten-181 and iridium-192 sources can be used to assess the viability of these seeds for brachytherapy treatments. Monte Carlo N-Particle 6 software, a tungsten-181 radioactive seed can be virtually simulated to find the geometry factors and dose rate constant required to calculate the radial dose function. The photon energies can be measured at different increments of 0.500 cm away from the source, all the way to 10 cm away, highlighting the drop off of energies the further away radiation is measured from the source. After obtaining the radial dose function of the simulated tungsten source, it can be compared directly to the radial dose function of an iridium-192 source, to determine its clinical viability. While the simulated tungsten has a relatively consistent radial dose function when taken at different distances away from the source, iridium-192 differentiates less across the same range. This is indicative of an iridium-192 having overall less absorption and less scattering than the Tungsten-181. While tungsten-181 could be viable in some applications, iridium-192 continues to be the best option for brachytherapy cancer treatments.

## **Acknowledgement**

I would like to thank my project advisor, Professor David Medich, for advising my project and guiding my research.

Thank you to PhD candidate, Matthew Jalbert, for helping me install, learn, and understand MCNP6.

Thank you to PhD candidate, Norbert Hugger, for assisting me resolve my coding issues and for assisting run computationally demanding code.

## Table of Contents

<b>Abstract</b>	<b>i</b>
<b>Acknowledgment</b>	<b>ii</b>
<b>1 Introduction</b>	<b>1</b>
<b>1.1 Measuring Radiation</b>	<b>1</b>
<b>1.2 High Dose Radiation</b>	<b>3</b>
<b>1.3 Brachytherapy</b>	<b>3</b>
1.3.1 Introduction	3
1.3.1 Radiation Sources Currently Being Used	5
<b>1.4 Tungsten 181</b>	<b>9</b>
<b>2 Methods</b>	<b>12</b>
<b>2.1 MCNP6</b>	<b>12</b>
<b>2.2 Experiment Setup</b>	<b>13</b>
2.2.1 Cell Cards	13
2.2.2 Surface Cards	14
2.2.3 Data Cards	16
2.2.4 Source Definitions	17
2.2.5 Material Definitions	18
<b>2.3 Experiment Procedure</b>	<b>19</b>
<b>3 Results</b>	<b>19</b>
<b>3.1 Geometry Function</b>	<b>19</b>
<b>3.2 Dose Rate Constant</b>	<b>21</b>
<b>3.3 Radial Dose Function</b>	<b>21</b>
<b>4 Analysis</b>	<b>23</b>

<b>5 Conclusion</b>	<b>25</b>
<b>References</b>	<b>26</b>
<b>Appendix A</b>	<b>29</b>
<b>Appendix B</b>	<b>30</b>
<b>Appendix C</b>	<b>31</b>

## **1 Introduction**

This paper will evaluate tungsten-181 for its dosimetric distributions to assess its viability for clinical applications in high dose rate brachytherapy. This paper compares the isotopes tungsten-181 and iridium-192 as radioactive sources for HDR brachytherapy. As brachytherapy continues to become a more widely adopted cancer treatment, it is important to explore as many applications, methods, and materials to maximize the treatment's potential. The purpose of this analysis is to provide valuable information to aid in the selection process of brachytherapy treatments. The small size of iridium-192 isotope and ease in which it is created have long since made it the standard source used in brachytherapy. However, there still are risks associated with isotope and the high energy photons emitted required special precautions to ensure proper radiation safety. The low energy x-ray source tungsten-181 could be presented as a viable alternative to iridium-192.

### **1.1 The Measurement of Radiation**

Four metrics are used to quantify a radioactive source; these metrics are radioactivity, exposure, effective dose, and absorbed dose. Radioactivity refers to the amount of ionizing radiation released by any given material in the form of emitted alpha or beta particles, gamma rays, x-rays, or neutrons. Exposure is the amount of radiation-produced ionization occurring in the air at a given location from the source. Absorbed dose is defined as the amount of energy deposited in a given material or medium as it passes through said material. An absorbed dose of 1 rad is equivalent to saying that 1 gram of material absorbed 100 ergs of energy. When measuring absorbed dose, the international system unit for measurement is known as the gray (Gy) which is

equivalent to 100 rad. (United States Nuclear Regulatory Commission, 2021). Effective dose is a modification of radiation absorbed that considers the potential biological risks associated with exposure to that source. (United States Nuclear Regulatory Commission, 2020).

Absorbed doses play an important role in finding the dose distributions of given radioactive materials. This information is then used in the medical physics quantity “radial dose function” to better understand the dosimetric interplay between radiation and scatter. As such, the radial dose function is defined as a quantity of the relative dose change resulting from photon attenuation and scatter in the medium along a source's central transverse axis. This function is influenced by filtration of photons through the use of encapsulation and different source materials, and can be calculated using Eq. 1 below. (Yue, 2013).

$$g_x(r) = \frac{\dot{D}(r, \theta_0)}{\dot{D}(r_0, \theta_0)} \cdot \frac{G_x(r_0, \theta_0)}{G_x(r, \theta_0)} \quad (1)$$

Here,  $\dot{D}(r, \theta_0)$  is the dose rate at point at a given radius,  $r$ , along the transverse axis where  $\theta$  is equal to  $\pi/2$ .  $\dot{D}(r_0, \theta_0)$  is the dose rate at the reference point ( $r_0 = 1$  cm,  $\theta_0 = \pi/2$ ),  $G_x(r_0, \theta_0)$  is the geometry factor at the reference point ( $r_0, \theta_0$ ), and  $G_x(r, \theta_0)$  at a given point on the transverse axis. The geometry factor accounts for variations in relative dose as a result of the spatial distribution of activity within a particular source. The geometry factor ignores both photon absorption and scattering in the source structure. When approximating a line source, as is the case in brachytherapy pellets, the geometry factor is defined as follows:

$$G(r, \theta) = \frac{\beta}{L r \sin\theta} \quad (2)$$

Where  $\beta$  is the angle subtended by the active source with respect to the reference point ( $r, \theta$ ), and  $L$  is the active length of the given source. (Nath et al., 1995). The radial dose function is a good

metric to look at when evaluating the effectiveness of a potential treatment, highlighting the falloff of a dose rate as the distance away from the given source is increased.

## **1.2 High Dose Radiation**

Radioactive materials are strictly monitored and regulated to prevent people from being inadvertently exposed or to ensure the safety of medical procedures. This is because high radiation doses have been shown to destroy cells, particularly when exposed over a short duration of time. Generally, the higher the dose of radiation, the faster the effects of the radiation will be exhibited, greatly increasing the probability of death. As the scientific community's understanding of high dose radiation has increased, so has the number of positive applications for said radiation. (United States Nuclear Regulatory Commission, 2020). The medical world has therefore developed a wide variety of applications for high dose radiation including radiotherapy treatments for numerous cancers.

## **1.3 Brachytherapy**

### **1.3.1 Introduction**

Brachytherapy is a type of internal radiation-based cancer treatment involving encapsulated radioactive sources. The sources are either inserted directly into or near the cancerous tissue. The radiation given off by the sources damages the DNA of the surrounding cancer cells, ultimately resulting in the destruction of the cancerous tissue. (Memorial Sloan Kettering Cancer Center, 2022). Brachytherapy allows doctors to precisely administer higher doses of radiation to particular parts of the body, when compared to conventional forms of radiation treatment such as external beam radiation. Rather than projecting radiation from an external machine into the body,

brachytherapy places sources directly into the affected areas, causing less damage and side effects to surrounding healthy tissue. (Mayo Clinic, 2020).

Brachytherapy is the most commonly used in the treatment of cancer in the prostate and has been used to treat a wide variety of other cancers including gynecologic, uterine, breast, lung, rectal, eye, and skin cancers. In most brachytherapy procedures, radiation sources are inserted into or near the cancerous tissue via a needle or catheter by a qualified radiation oncologist. The methods in which radioactive materials are inserted into the body are dependent on the type of cancer the patient is afflicted with. (Memorial Sloan Kettering Cancer Center, 2022).

Brachytherapy can be divided into three distinct types of implants. These categories are low-dose rate (LDR) implants, high-dose rate (HDR) implants, and permanent implants. In LDR implants, radiation sources remain implanted anywhere between 1 to 7 days. As for HDR implants, radiation sources are only left in the body between 10 to 20 minutes before being promptly removed. These treatments can range from twice a day for only 2 to 5 days to a once weekly treatment over the duration of 2 to 5 weeks. This schedule is heavily dependent on the particular cancer attempted to be treated. The final type of brachytherapy: permanent implant, is not like the other types in that once this radiation source is placed within the body, the catheter is removed, and the source remains embedded in the patient. This radiation source is designed to remain in the body for the rest of the patient's life, as the radiation continues to get weaker day by day. In the case of permanent implants, it is important to limit time spent around other people initially as a safety precaution. (National Cancer Institute, 2019).

### 1.3.2 Radiation Sources Currently Being Used

There are several radioactive sources that are currently being used in brachytherapy. Some of these include iridium-192, iodine-125, and palladium-103. These radioactive sources are utilized due to their short half-lives: 74.17 days, 60.25 days, and 16.96 days respectively. These radionuclides can be left within the body after being inserted, becoming stable forms relatively quickly. (L'Annunziata, 2016). Of the radioisotopes previously mentioned, iridium-192 is regarded as the gold standard for high-dose rate brachytherapy. It is the most commonly used isotope due to it having a both high and low dose rates depending on the concentration of iridium-192, its relative ease to manufacture, its small source size, its stable daughter product, and its ability to be reusable. When iridium-192 is used in LDR treatment the source is implanted in the form of temporary wires or needles, while remote afterloading techniques are used for iridium-192 HDR treatments. Iridium-192 is produced via neutron bombardment of a stable iridium-191 and then is alloyed with platinum in the form of a wire. This wire is coated in platinum in order to effectively filtrate the electrons produced by the iridium decaying. This process is relatively easy to perform because of the availability of pure iridium-191, and minimally produces unwanted isotopes as well as having a large cross section for neutron interactions. (Nikoofar et al., 2015). Thus, in order to evaluate the potential effectiveness of the tungsten-181 isotope, we will compare its radial dose function to the radial dose function of iridium-192. The photon energies and emission rates can be found in table 1 below.

<b>Table 1. Ir-192 Photon Energies &amp; Emission Rates</b>	
<b>Photon Energies (keV)</b>	<b>Emission Rates (%)</b>
7.822	0.028

*Marquez: Major Qualifying Project*

---

8.266	0.076
8.840	0.064
8.911	0.57
9.337	0.0087
9.362	0.166
9.443	1.47
9.975	0.0271
10.176	0.042
10.217	0.0078
10.354	0.408
10.511	0.058
10.590	0.133
10.840	0.0211
10.854	0.056
10.871	0.0075
11.071	1.24
11.235	0.073
11.242	0.354
11.562	0.0292
12.096	0.079
12.385	0.0066
12.422	0.0133
12.500	0.019
12.942	0.245
13.271	0.030

Marquez: Major Qualifying Project

---

13.273	0.018
13.361	0.025
60.903	0.00106
61.486	1.20
63.000	2.07
64.514	0.00286
65.122	2.65
66.831	4.53
71.079	0.239
71.414	0.460
71.875	0.0113
73.363	0.162
73.590	0.0188
75.368	0.533
75.749	1.029
76.233	0.0265
77.831	0.365
78.073	0.0478
110.093	0.0126
136.34348	0.183
176.98	0.0043
201.3112	0.472
205.79549	3.300
214.7	<0.0026
214.7	<0.0026

280.04	0.023
283.2668	0.262
295.95827	28.67
308.45692	30.00
314.8	<0.07
314.8	<0.07
316.50791	82.81
329.312	0.0185
374.4852	0.721
415.4	<0.009
415.4	<0.009
416.4714	0.664
420.532	0.0737
468.07152	47.83
484.5780	3.184
485.30	0.0022
489.039	0.443
588.5845	4.515
593.37	0.0426
599.35	0.0039
604.41464	8.23
612.46564	5.309
703.98	0.0053
739	<0.00050
739	<0.00051

765.8	0.00149
884.5418	0.2923
1061.48	0.0528
1089.7	0.00108
1378.3	0.00124

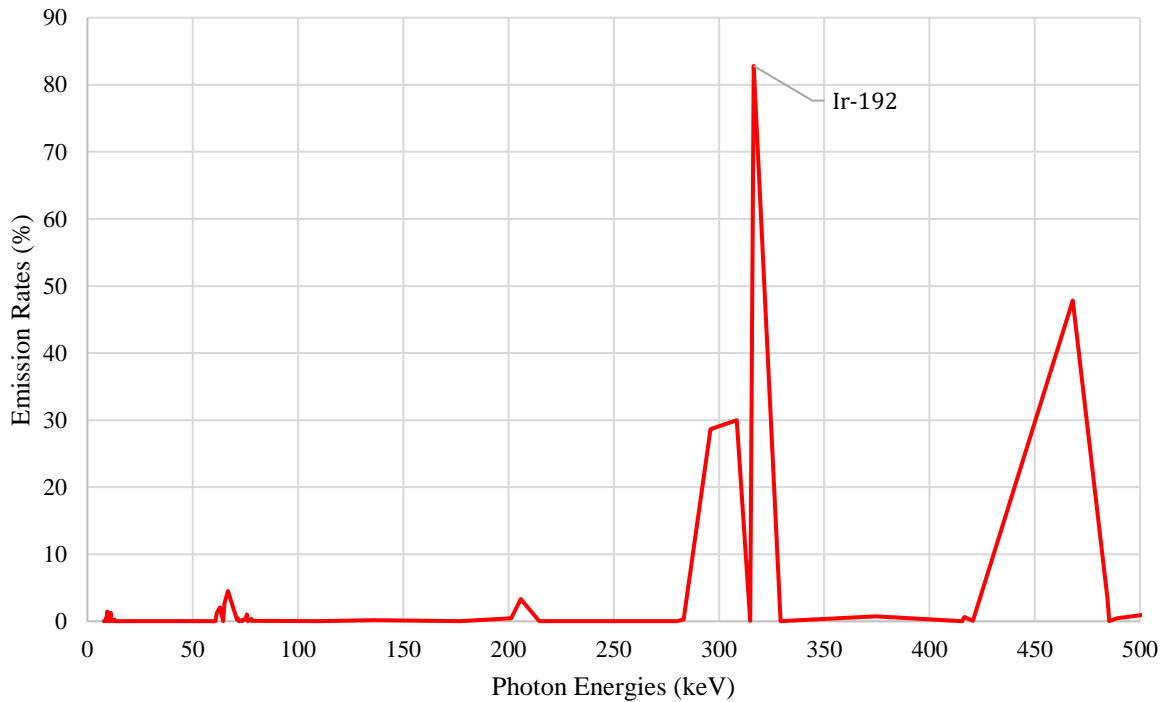


**Figure 1.** Iridium-192 Photon Energies & Emission Rates

## 1.4 Tungsten-181

Tungsten, atomic number 74, is a heavy and hard metal found in numerous ores including wolframite and scheelite. There are 5 stable isotopes that occur in natural tungsten, and 21 unstable isotopes. (Bradford, 2020). Stable tungsten isotopes can be enriched in order to produce more unstable isotopes with more useful medical applications. Tungsten-180 is used in the production of the therapeutic radioisotope tungsten-181 through the process of neutron capture. (Cork,1953).

A total of 27 artificial radioisotopes of tungsten have been characterized thus far by the scientific community, with tungsten-181 being the most stable with a half-life of 121.2 days. (McGill, n.d.). The main form of decay of tungsten-181 occurs via K capture and decays directly into the ground state of tantalum- 181. (Cork, 1953). The isotope's short half-life would allow a potential tungsten-181 brachytherapy seed to be left within the body after being inserted into cancerous tissue. (L'Annunziata, 2016). Additionally, tungsten-181 has a very low photon energy emission, which would potentially make it safer than other options currently being implemented in medical applications. This means a potential tungsten-181 brachytherapy seed would require less shielding to be utilized in a medical setting. For these reasons, tungsten-181's clinical viability should be evaluated.

<b>Table 2. W-181 Photon Energies and Emission Rates</b>	
<b>Photon Energies (keV)</b>	<b>Emission Rates (%)</b>
7.173	0.35
8.088	0.85
8.146	7.6
8.428	0.113
9.213	1.02
9.316	0.093
9.343	5.4
9.488	1.48
9.646	1.67
9.875	0.0303
10.895	1.00
11.130	0.0259

11.217	0.32
11.277	0.46
55.735	0.0131
56.280	18.7
57.535	32.6
64.948	3.62
65.222	6.98
65.652	0.158
66.982	2.40
67.181	0.372

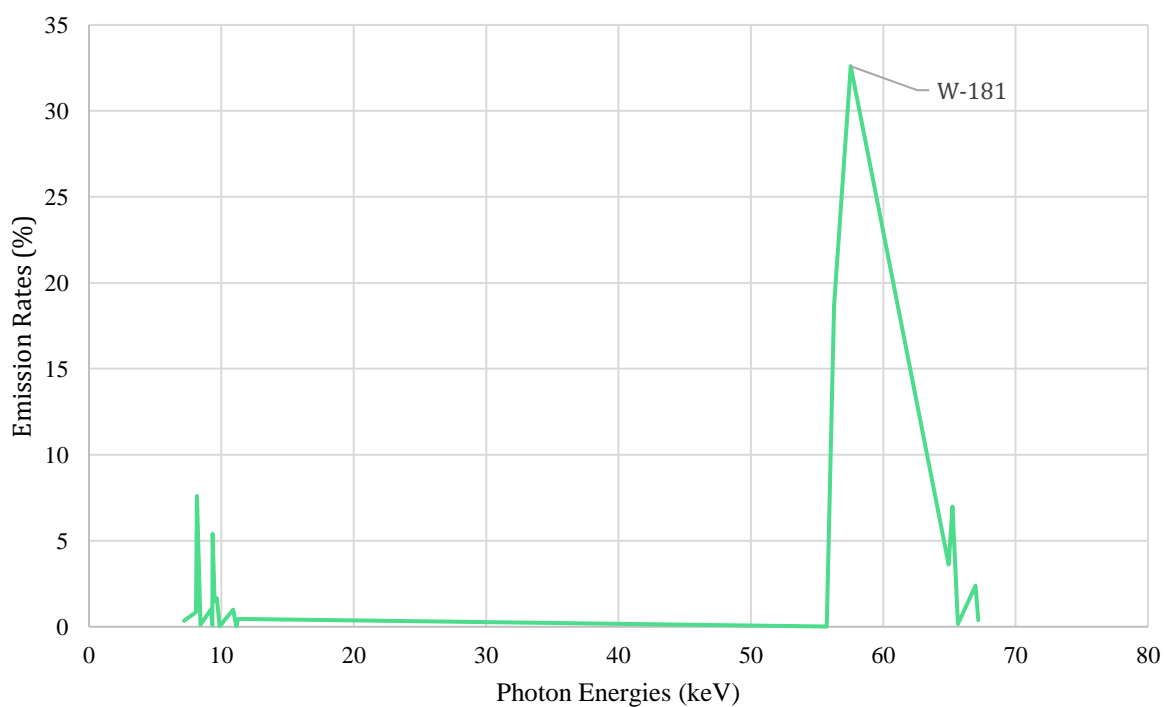


**Figure 2.** W-181 Photon Energies & Emission Rates

The photon energies and emission rates of tungsten-181 and iridium-192 are directly compared to one another in figure 3.

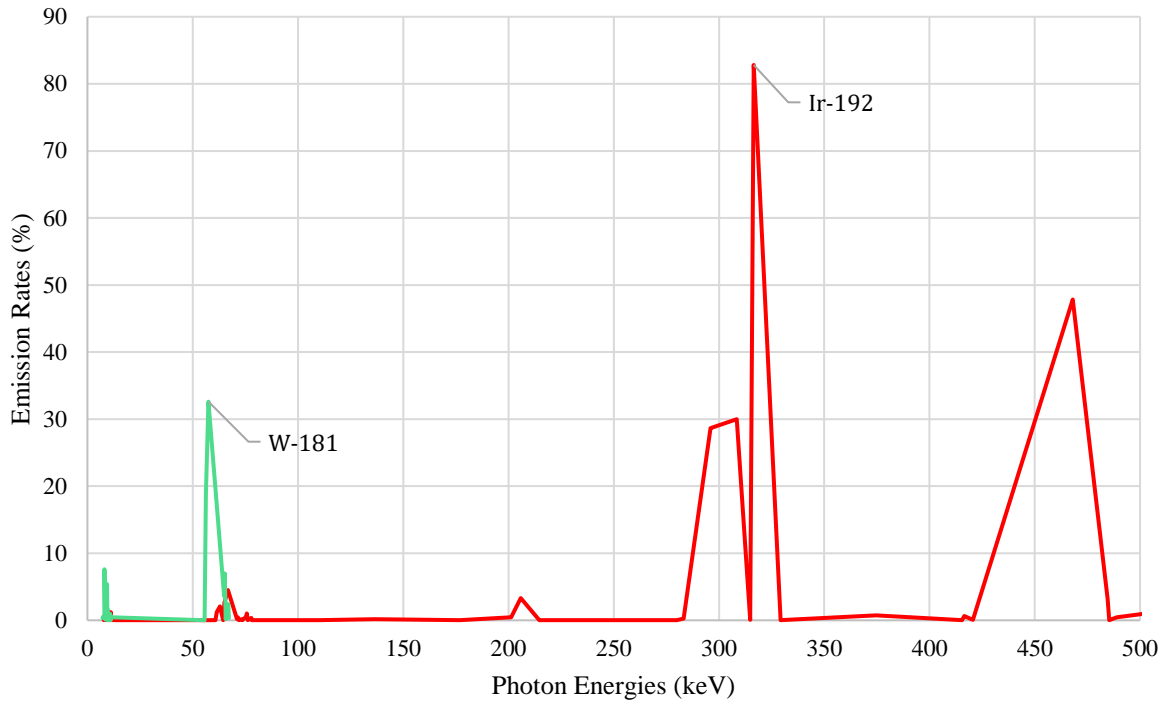


**Figure 3.** W-181 VS. Ir-192 Photon Energies & Emission Rates

## 2 Methods

### 2.1 MCNP6

The Monte Carlo N-Particle (MCNP6) program has been chosen to analyze tungsten-181 as a viable HDR brachytherapy radiation source, due to the software’s ability to model radioactive particles and systems they interact with. MCNP6 is a general-purpose code that can be utilized to create neutron, photon, electron, or combined neutron, photon, and electron simulation. The code has several applications including areas such as radiation protection, dosimetry, radiation shielding, radiography, medical physics, nuclear criticality safety, as well as fissions and fusion reactor design, decontamination, and decommissioning. (Los Alamos National Laboratory, 2022).

## **2.2 Experiment Setup**

To effectively simulate the viability of tungsten-181, a simulated brachytherapy pellet needs to be created within MCNP, including the radiation source, the material it is encapsulated, and a simulated fleshed needed to be created in the form of a water phantom. To have these elements be properly represented in the program, several components need to be defined within the code. The components include cell cards, surface cards, data cards, source definitions, and materials. In addition to these components, the boundaries of the simulated world need to be defined to conserve computational demand when running the code. The end of the simulated world can be created in the cell cards as well. Similarly, the number of particles simulated will be set to 50,000,000 to keep computations reasonable and accurate, without succumbing to the computational demands of running such large simulations.

### **2.2.1 Cell Cards**

When creating cell cards in MCNP6, the cell number is the first entry listed. The second entry listed is the arbitrarily assigned cell material number. This number references the materials later defined. After the material number has been defined, the cell material density is next. The following entry can be defined as the entire specification of the cell's geometry. After this, the importance of the region is defined to photons and electrons. Four cell cards need to be defined: the tungsten-181 pellet, the aluminum capsule, the water phantom, and the end of world.

The tungsten-181 pellet cell number is 10. The material number is 3. The cell material density is  $19.00 \text{ g/cm}^3$ . The specific geometry is bounded from -116, -119, 118. Finally, the cell has a photon and electron importance of 1. (See Appendix A for tungsten-181 pellet cell card).

The aluminum capsule is made of three separate cells. These cells have the numbers 20, 30, and 40. Cell 20 has a material number of 2, a cell material density of  $2.70 \text{ g/cm}^3$ , the specific geometry is bound from -116, -118, 218, and the cell has a photon and electron importance of 1. Cell 30 has a material number of 2, a cell material density of  $2.70 \text{ g/cm}^3$ , the specific geometry is bound from -116, 119, -219, and the cell has a photon and electron importance of 1. Cell 40 has a material number of 2, a cell material density of  $2.70 \text{ g/cm}^3$ , the specific geometry is bound from -216, 116, -219, 218, and the cell has a photon and electron importance of 1. (See Appendix A for aluminum capsule cell card).

Similar to the aluminum capsule, the water phantom is also composed of three separate cells. Cell 50 has a material number of 1, a cell material density of  $1 \text{ g/cm}^3$ , the specific geometry is bound from -218, -400 and the cell has a photon and electron importance of 1. Cell 60 has a material number of 1, a cell material density of  $1 \text{ g/cm}^3$ , the specific geometry is bound from 219, -400 and the cell has a photon and electron importance of 1. Cell 70 has a material number of 1, a cell material density of  $1 \text{ g/cm}^3$ , the specific geometry is bound at 218, -219 216 -400 and the cell has a photon and electron importance of 1. (See Appendix A for water phantom cell card).

The end of world cell is defined as 999. The cell material is 0. There is no cell material density. The specific geometry is bound at 400 and the cell has a photon and electron importance of 0. (See Appendix A for end of world cell card).

### **2.2.2 Surface Cards**

When creating surface cards in MCNP6, the surface number is the first entry listed. The next entry listed is an alphabetic mnemonic that denotes the surface type present. Some of these

mnemonics in PX, PY, PZ, CZ, and SO. This experiment is only concerned with the z-axis, so PZ, CZ, and SO are the only mnemonics relevant to the surface cards in this simulation. Following the surface type are the numerical coefficients associated with the equational representation of the surface. Three surface cards need to be defined: the tungsten-181 pellet, the aluminum capsule, and the end of world.

The tungsten-181 pellet card is comprised of three surfaces. Surface 116 is defined as a cylinder on the Z-axis denoted by CZ and is located at 0.03250. Surface 118 is defined as a plane normal to the Z-axis surface denoted by PZ and is located at -0.18750. Surface 119 is defined as a plane normal to the Z-axis surface denoted by PZ and is located at 0.18750. (See Appendix B for tungsten-181 pellet surface card).

Similar to the tungsten-181 pellet, the aluminum capsule card is made up of three separate surfaces. Surface 216 is defined as a cylinder on the Z-axis denoted by CZ and is located at 0.05250. Surface 218 is defined as a plane normal to the Z-axis denoted by PZ and is located at -0.20750. Surface 219 is defined as a plane normal to the Z-axis denoted by PZ and is located at 0.20750. (See Appendix B for aluminum capsule surface card).

The end of world card has surface number 400, a spherical surface type centered around the origin, indicated by the SO mnemonic, and is located at 142.0. (See Appendix B for end of world surface card).

### 2.2.3 Data Cards

When creating data cards in MCNP6, five subcards are essential to define to run the simulation without issue. These elements include the mode, tally, history, source, and material cards.

The mode card is used to denote the kind of problem the software will be solving by indicating the type of source particles that are being tracked. In the case of this simulation, mode “p” is used to represent photon energies. (See Appendix C for mode card).

The tally card is used to determine how the results of the simulation will be compiled, measured, and recorded. The FMESH4 command can be used to take a track-length tally over a given 3-dimensional mesh. In the case of this simulation, the 3-dimensional geometry mesh is a cylinder with an origin simulated at 0 0 0. Using the “mesh” and “ints” prompts in MCNP allows a user to specify where measurements will be recorded across the x, y, and z axes. IMESH represents the boundaries of tally bins across the i-direction vector. To find the doses at even increments of 0.500 cm, the boundaries of the tally bin are taken 0.25 cm above and below the desired increment found at the midpoint between the two edges of the bin. The code allowing this is  $IMESH = 0.25 \ 10.25$ . IINTS represents the number of integers where calculations will be recorded at. To collect data increments of 0.500 cm, we can take a total of 21 values starting at 0.125 cm to this properly. For our simulation,  $IINTS = 1 \ 20$ . JMESH represents the boundaries of the tally bins across the j-direction vector. J is a measure of length and in the case of this simulation, the cylinder thickness is 1 mm thick represented by  $JMESH = 0.1$ . JINTS represents the number of integers where calculations will be recorded at. Because the thickness of the cylinder is uniform throughout the surface, thus,  $JINTS = 1$ . KMESH represents the boundaries of the tally bin across

the k-direction vector. For the purposes of this simulation,  $KMESH = 1$ .  $KINTS$  represents the number of integers where calculations will be recorded at. To collect data in  $10^\circ$  increments, all the way around a full  $360^\circ$  rotation around the source. Thus, the code can be written as  $KINTS = 36$ . (See Appendix C for tally card).

To prevent the simulation from running indefinitely, the histories card is used to stop this from occurring, keeping the number of source particle histories simulated to a specified amount. The maximum number of histories is denoted by “nps n” where n is the number of histories specified in the card. In the case of this simulation, 50,000,000 source particle histories were simulated to reduce error and ensure more accurate calculated values. (See Appendix C for histories card).

#### **2.2.4 Source Definitions**

When defining sources in MCNP6, it is important to use the SDEF command to properly define all aspects and parameters of the source. This allows all the characteristics of the particular source to be properly simulated within the software. SDEF consists of several components: PAR, POS, RAD, AXS, EXT, and ERG. Throughout the code any distribution of values is represented by dn, where n is a given integer assigned to distribution.

PAR represents the type of particle source emitted in the given simulation. In the case of this simulation,  $PAR = 2$ , denoting the particles are photons. POS represents the position of the reference point being used for sampling. The position of the reference point in the code is denoted by  $POS = d1$ . RAD represents the radial distance of the position away from either the POS or the AXS. In this simulation,  $RAD = d2$ . AXS represents the reference vector for both RAD and EXT

values. The value used in this code is  $AXS = 0\ 0\ 1$ . EXT represents the distance from the POS along the AXS in instances of the cell case. We have an  $EXT = d3$ . Finally, ERG simply represents the energy given in units of MeV. The energy used in this simulation is  $ERG = d4$ .

Also defined within the source card are the values referred to as the source information, denoted by “SI,” and the source probability, denoted by “SP.” This information is presented in a column format, with the energies of tungsten-181 and the emission rates associated with those energies being compiled so they can be drawn from later while running the simulation. (See Appendix C for source definitions).

### **2.2.5 Material Definitions**

When defining materials cards in MCNP6, the first element entered is the unique material number. This value is then followed by the given material’s elemental or isotopic composition. The final element that is required is the cross section compilations that are expected to be used during the simulation. The three materials used in the simulation are denoted by m1, m2, and m3. Material m1 represents the water molecules present within the phantom, composed of 2 hydrogen atoms and 1 oxygen atom. This ratio of hydrogen and oxygen in water is written as a percentage of 1 after the atomic number of each element, 0.6667 and 0.3333 respectively. Material m2 represents the aluminum capsule, uniformly composed of aluminum atoms. Finally, material m3 represents the tungsten-181 brachytherapy seed, uniformly composed of tungsten atoms. (See Appendix C for material definitions).

## 2.3 Experiment Procedure

To evaluate tungsten-181 for viable use in medical treatments, we will use the MCNP code to evaluate the absorbed dosimetric distributions from a tungsten-181 pellet and calculate its radial dose profile. These results will then be compared against the radial dose profile of iridium-192, which is the current gold standard of HDR brachytherapy. The MCNP6 command prompt window can be used in order to successfully execute the created tungsten-181 brachytherapy simulation. The data is then exported into two .txt documents denoted by “out” and “meshta” respectively.

## 3 Results

After the MCNP simulation is effectively executed, two .txt files were created which compile the necessary data to continue further calculations using the radial dose function which is evaluated along the transverse axis. We can take  $\theta_0$  to be  $\pi/2$  and take the starting radius  $r_0$  to be 1 cm. Using the line-source approximation to model the geometric falloff of the photon fluence, the radial dose function was obtained at increments of 0.5 cm, up until a distance of 10 cm. Using these values, the line-source approximations, and their respective geometry factors we can determine tungsten-181’s radial dose profile to compare it to the radial dose profile of iridium-192. The calculations are in the tables below.

### 3.1 Geometry Function

The geometry function was calculated using Eq. 2 for a 7 mm long brachytherapy seed, which results in the geometry function present in Table 3 and displayed graphically in Figure 4.

<b>Table 3. Geometry Function <math>G(r, \theta)</math></b>	
<b>r (cm)</b>	<b><math>G(r, \theta)</math></b>
0.125	28.0634
0.500	3.4899
1.000	0.9619
1.500	0.4366
2.000	0.2475
2.500	0.1590
3.000	0.1106
3.500	0.0814
4.000	0.0623
4.500	0.0493
5.000	0.0399
5.500	0.0330
6.000	0.0277
6.500	0.0236
7.000	0.0204
7.500	0.0178
8.000	0.0156
8.500	0.0138
9.000	0.0123
9.500	0.0111
10.00	0.0100

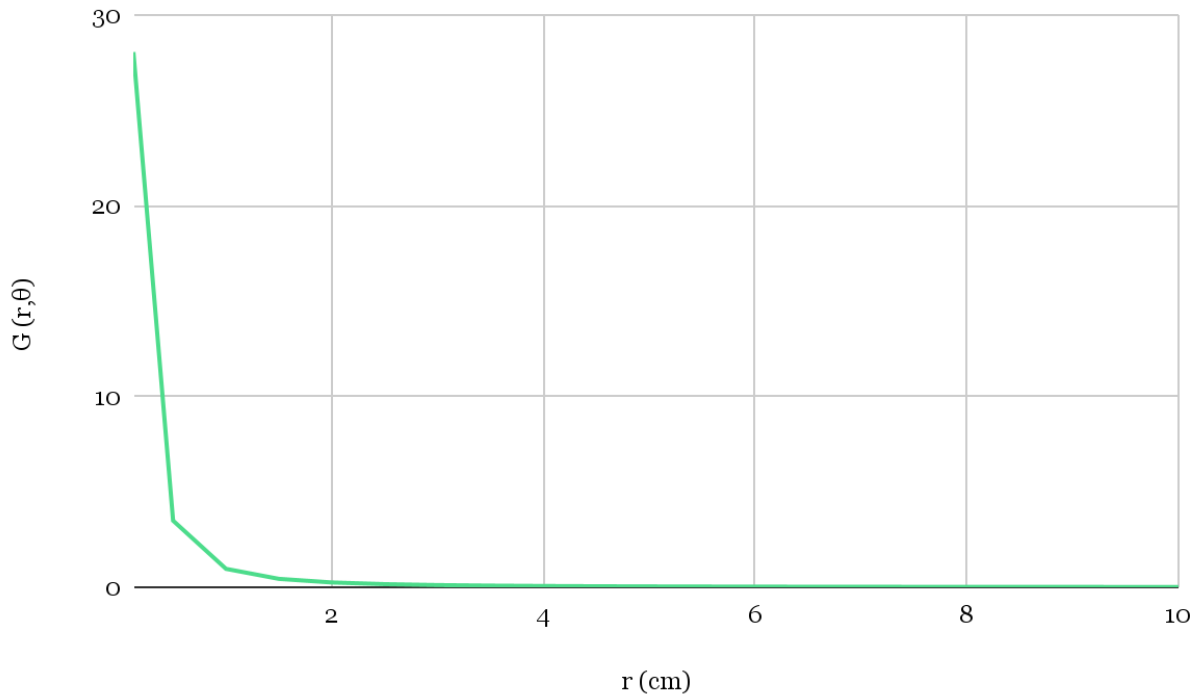


**Figure 4.** Geometry Factor VS. Distance

### 3.2 Dose Rate Constant

To calculate the radial dose function properly, it is important to first determine the dose rate constant. This value is the dose rate measured at an angle of  $90^\circ$  1 cm away from the source. This value was found by using Eq. 1 and determined to be 0.103 for this tungsten-181 source.

### 3.3 Radial Dose Function

Using Eq. 1, the dose rate constant, the geometry functions, and the simulated doses to calculate the radial dose function as measured incrementally further and further away from the source to produce the radial dose function of the source, which is presented in Table 4 and displayed graphically in Figure 4.

**Table 4. Radial Dose Function  $g(r)$**

<b>r (cm)</b>	<b>Dose</b>	<b><math>g(r)</math></b>	<b>Uncertainty of <math>g(r)</math></b>
0.125	3.47	1.152	0.036
0.500	0.419	1.117	0.036
1.000	0.103	1.000	0.036
1.500	0.0455	0.968	0.036
2.000	0.0254	0.954	0.036
2.500	0.0161	0.944	0.036
3.000	0.0112	0.938	0.036
3.500	0.00813	0.929	0.036
4.000	0.00619	0.924	0.037
4.500	0.00486	0.917	0.037
5.000	0.00391	0.910	0.037
5.500	0.00320	0.901	0.037
6.000	0.00266	0.893	0.037
6.500	0.00225	0.887	0.037
7.000	0.00193	0.883	0.037
7.500	0.00168	0.879	0.037
8.000	0.00147	0.876	0.038
8.500	0.00129	0.870	0.038
9.000	0.00115	0.863	0.038
9.500	0.00102	0.857	0.038
10.00	0.000913	0.761	0.038

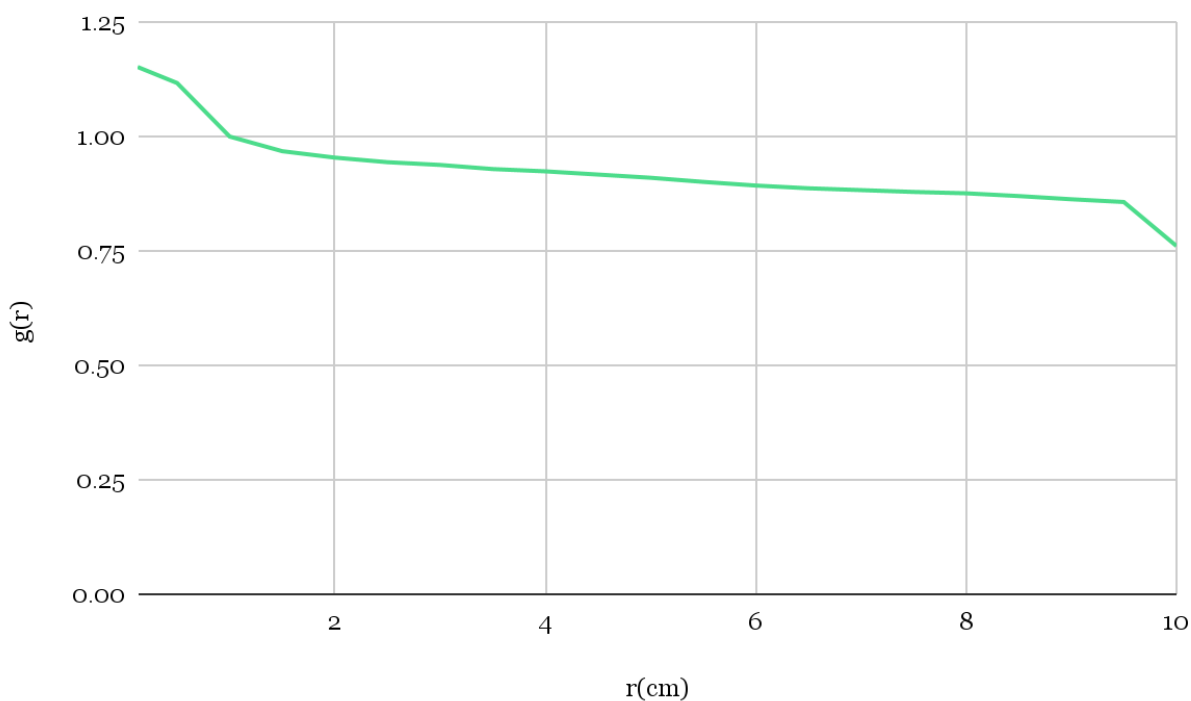


**Figure 5.** Radial Dose Function VS. Distance

To ensure that the simulations are as accurate as possible, a total of 50,000,000 particles were simulated, resulting in relatively low margins of error, all below 5%, as shown in the “Uncertainty  $g(r)$ ” column of the table above. To calculate the uncertainty of  $g(r)$ , uncertainties and relative errors were collected throughout the process of recording measurements, both simulated and calculated. Using the methodology and equations derived published in the 2005 journal, *Medical Physics*, volume 33, issue 1. (Medich et al., 2005).

## 4 Analysis

After completing our radial dose calculations for tungsten-181, we can compare it to the radial dose profile of iridium-192 to evaluate if tungsten-181 would make a viable brachytherapy. The radial dose functions of tungsten-181 and iridium-192 as measured at 0.500 cm increments

along a distance of 10 cm are found in table 5 below.

<b>Table 5. Tungsten-181 &amp; Iridium-192 Radial Dose Function Comparison</b>		
<b>Distance r (cm)</b>	<b>Radial Dose Function of Tungsten-181</b>	<b>Radial Dose Function of Iridium-192</b>
0.125	1.152	-
0.500	1.117	0.995
1.000	1.000	1.000
1.500	0.968	1.003
2.000	0.954	1.006
2.500	0.944	1.007
3.000	0.938	1.009
3.500	0.929	1.009
4.000	0.924	1.008
4.500	0.917	1.007
5.000	0.910	1.005
5.500	0.901	-
6.000	0.893	0.998
6.500	0.887	-
7.000	0.883	0.988
7.500	0.879	-
8.000	0.876	0.975
8.500	0.870	-
9.000	0.863	0.959
9.500	0.857	-
10.00	0.761	0.942

## **5 Conclusion**

A dosimetric study of a hypothetical HDR tungsten-181 brachytherapy source was conducted using MCNP6 code simulation. The radial dose function of tungsten-181 ranges from 1.152 to 0.761 across increments measured up to 10 cm away from the radioactive source. Over the same distances away from an iridium-192 brachytherapy seed source only ranges 1.009 to 0.942. Overall, this indicated there is less absorption and less scattering in the iridium-192 sample source. While the low energy x-ray tungsten-181 could still be viable for certain cancer treatments, iridium-192 still remains a more advantageous source for brachytherapy.

## References

- AAPM: *The American Association of Physicists in Medicine*. (n.d.). Retrieved April 27, 2023, from [https://aapm.org/pubs/reports/RPT\\_41.pdf](https://aapm.org/pubs/reports/RPT_41.pdf)
- Brachytherapy (HDR & LDR)*. UCSF Department of Radiation Oncology. (2021, April 28). Retrieved April 27, 2023, from <https://radonc.ucsf.edu/conditions-treatments/types-of-treatment/brachytherapy-hdr-ldr/>
- Brachytherapy*. Brachytherapy - an overview|ScienceDirect Topics. (n.d.). Retrieved April 27, 2023, from <https://www.sciencedirect.com/topics/physics-and-astronomy/brachytherapy#:~:text=Some%20radioactive%20sources%20used%20for,cancerous%20tumor%20and%20never%20removed.>
- Brachytherapy for Cancer*. National Cancer Institute. (n.d.). Retrieved August 9, 2022, from <https://www.cancer.gov/about-cancer/treatment/types/radiation-therapy/brachytherapy#:~:text=Brachytherapy%20is%20a%20type%20of%20internal%20radiation%20that%20uses%20radiation,in%20or%20near%20the%20cancer.>
- Bradford, A. (2020, February 3). *Facts About Tungsten*. livescience.com. Retrieved December 15, 2022, from <https://www.livescience.com/38997-facts-about-tungsten.html>
- Buchapudi, R. R., Manickam, R., & Chandaraj, V. (2019). *Experimental determination of radial dose function and anisotropy function of gammamed plus 192Ir high-dose-rate brachytherapy source in a bounded water phantom and its comparison with Egs brachy Monte Carlo Simulation*. *Journal of medical physics*. Retrieved April 27, 2023, from <https://www.ncbi.nlm.nih.gov/pmc/articles/PMC6936200/>
- Calcina, C. S. G., Almeida, A. D., Rocha, J. R. O., Abrego, F. C., & Baffa, O. (2005). Ir-192 HDR transit dose and radial dose function determination using alanine/EPR dosimetry. *Physics in Medicine and Biology*, 50(6), 1109–1117. <https://doi.org/10.1088/0031-9155/50/6/005>
- Cork, J. M. (1953, October 1). *The Radioactive Decay of Tungsten 181*. *Physical Review Journals Archive*. Retrieved December 15, 2022, from <https://journals.aps.org/pr/abstract/10.1103/PhysRev.92.119>
- Eye Physics. (n.d.). *Radial Dose*. Retrieved December 15, 2022, from <https://eyephysics.com/PS/PS6/UserGuide/Physics5RadialDose.html>
- IAEA. (2017, July 25). *Optimization in Brachytherapy*. IAEA. Retrieved April 27, 2023, from <https://www.iaea.org/resources/rpop/health-professionals/radiotherapy/brachytherapy/optimization>
- IEEE Xplore*. (n.d.). Retrieved April 27, 2023, from <https://ieeexplore.ieee.org/document/263008>
- Iridium 192*. (n.d.). Ozradonc. <http://ozradonc.wikidot.com/iridium-192>
- Iridium-192*. (n.d.). Advancing Nuclear Medicine. Retrieved December 20, 2022, from <https://www.advancingnuclearmedicine.com/products/iridium-192>

- L'Annunziata, M. F. (2016). *Radioactivity: Introduction and History, From the Quantum to Quarks* (2nd ed.). Elsevier.
- Learn about brachytherapy radiation cancer treatment.* Memorial Sloan Kettering Cancer Center. (n.d.). Retrieved August 9, 2022, from <https://www.mskcc.org/cancer-care/diagnosis-treatment/cancer-treatments/radiation-therapy/what-brachytherapy>
- Lund University. (n.d.). Periodic chart of the nuclides. Retrieved April 27, 2023, from <http://nucleardata.nuclear.lu.se/toi/perchart.htm>
- Mayo Foundation for Medical Education and Research. (2020, June 19). *Brachytherapy*. Mayo Clinic. Retrieved August 9, 2022, from <https://www.mayoclinic.org/tests-procedures/brachytherapy/about/pac-20385159>
- MCNP® Website.* (n.d.). Los Alamos National Laboratory. Retrieved September 7, 2022, from <https://mcnp.lanl.gov/>
- Mettler, F. A., & Upton, A. C. (2008). *Medical Effects of Ionizing Radiation*. Elsevier Gezondheidszorg.
- Nath, R., Anderson, L. L., Luxton, G., Weaver, K. A., Williamson, J. F., & Meigooni, A. S. (1995). Dosimetry of interstitial brachytherapy sources: Recommendations of the AAPM Radiation Therapy Committee Task Group No. 43. *Medical Physics*, 22(2), 209–234. <https://doi.org/10.1118/1.597458>
- NCI dictionaries.* National Cancer Institute. (n.d.). Retrieved April 27, 2023, from <https://www.cancer.gov/publications/dictionaries>
- NCI Dictionary of Cancer terms.* National Cancer Institute. (n.d.). Retrieved April 27, 2023, from <https://www.cancer.gov/publications/dictionaries/cancer-terms/def/high-dose-radiation>
- Nikoofar, A., Hoseinpour, Z., Rabi Mahdavi, S., Hasanzadeh, H., & Rezaei Tavirani, M. (2015). High-Dose-Rate <sup>192</sup>Ir Brachytherapy Dose Verification: A Phantom Study. *Iranian Journal of Cancer Prevention*, 8(3). <https://doi.org/10.17795/ijcp2330>
- Optimization in brachytherapy | IAEA.* (n.d.). International Atomic Energy Agency. Retrieved December 20, 2022, from <https://www.iaea.org/resources/rpop/health-professionals/radiotherapy/brachytherapy/optimization>
- Paul, R., Hofmann, R., Schwarzer, J. U., Stepan, R., Feldmann, H. J., Kneschaurek, P., Molls, M., & Hartung, R. (1997). Iridium 192 high-dose-rate brachytherapy ?a useful alternative therapy for localized prostate cancer? *World Journal of Urology*, 15(4), 252–256. <https://doi.org/10.1007/bf01367663>
- S;, N. (n.d.). *High dose rate brachytherapy: Its clinical applications and treatment guidelines.* Technology in cancer research & treatment. Retrieved April 27, 2023, from <https://pubmed.ncbi.nlm.nih.gov/15161320/>
- Tungsten.* Wikispeedia. (n.d.). Retrieved April 27, 2023, from <https://www.cs.mcgill.ca/~rwest/wikispeedia/wpcd/wp/t/Tungsten.html>

- United States Nuclear Regulatory Commission. (2020, March 20). *Measuring Radiation*. U.S. NRC. Retrieved December 20, 2022, from <https://www.nrc.gov/about-nrc/radiation/health-effects/high-rad-doses.html>
- United States Nuclear Regulatory Commission. (2020, March 20). *Measuring Radiation*. U.S. NRC. Retrieved December 15, 2022, from <https://www.nrc.gov/about-nrc/radiation/health-effects/measuring-radiation.html>
- United States Nuclear Regulatory Commission. (2021, March 9). *Rad (radiation absorbed dose)*. U.S. NRC. Retrieved December 15, 2022, from <https://www.nrc.gov/reading-rm/basic-ref/glossary/rad-radiation-absorbed-dose.html>
- World Nuclear Association. (2022, April). *Radioisotopes in Medicine | Nuclear Medicine*. Retrieved December 15, 2022, from <https://world-nuclear.org/information-library/non-power-nuclear-applications/radioisotopes-research/radioisotopes-in-medicine.aspx>
- Yue, N. J. (2013). *Radial Dose Function*. SpringerLink. Retrieved December 15, 2022, from [https://link.springer.com/referenceworkentry/10.1007/978-3-540-85516-3\\_309?error=cookies\\_not\\_supported&code=fdee00f3-0b29-413a-a1d9-2362fcb14c31](https://link.springer.com/referenceworkentry/10.1007/978-3-540-85516-3_309?error=cookies_not_supported&code=fdee00f3-0b29-413a-a1d9-2362fcb14c31)

## Appendix A

This appendix consists of the MCNP code necessary to run the cell card simulations.

```
c CELL CARDS
c Tungsten Pellet
10  3  -19.00  (-116 -119 118)      imp:p,e=1
c Al Capsule, bottom, top and shell
20  2  -2.70  (-116 -118 218)      imp:p,e=1
30  2  -2.70  (-116 119 -219)      imp:p,e=1
40  2  -2.70  (-216 116 -219 218)  imp:p,e=1
c Water Phantom
50  1  -1     (-218 -400)          imp:p,e=1
60  1  -1     (219 -400)           imp:p,e=1
70  1  -1     (218 -219 216 -400)  imp:p,e=1
c EOW
999  0          (+400)          imp:p,e=1
c End Cell Cards
```

## Appendix B

This appendix consists of the MCNP code necessary to run the surface card simulations.

c SURFACE CARDS

c Pellet

116 CZ 0.03250

118 PZ -0.18750

119 PZ 0.18750

c Capsule

216 CZ 0.05250

218 PZ -0.20750

219 PZ 0.20750

c EOW

400 SO 142.0

c End Surface Cards

## Appendix C

This appendix consists of the MCNP code necessary to run the multiple sections of the data card simulations. These sections include the tally section, tally section, source section, the materials section, and the histories section.

c DATA CARDS

mode p

c Tally Section

```
*FMESH04:p Geom = cyl Origin = 0 0 0
      AXS 1 0 0  VEC 0 0 1
      IMESH = 0.25 10.25  IINTS = 1 20
      JMESH = 0.1         JINTS = 1
      KMESSH = 1         KINTS = 36
      OUT = col
```

#	DE04	DF04
	0.0010	4065.00
	0.0015	1372.00
	0.0020	615.20
	0.0030	191.70
	0.0040	81.91
	0.0050	41.88
	0.0060	24.05
	0.0080	9.915
	0.0100	4.944
	0.0150	1.374
	0.0200	0.5503
	0.0300	0.1557
	0.0400	0.06947
	0.0500	0.04223

0.0600	0.03190
0.0800	0.02597
0.1000	0.02546
0.1500	0.02764
0.2000	0.02967
0.3000	0.03192
0.4000	0.03279
0.5000	0.03299
0.6000	0.03284
0.8000	0.03206
1.0000	0.03103
1.2500	0.02965
1.5000	0.02833

c Source Definition

```
sdef par=2 pos=d1 rad=d2 axs=0 0 1 ext=d3 erg=d4
```

```
si1 L 0 0 0
```

```
sp1 1.0000
```

```
si2 0.000 0.03250
```

```
sp2 -21 1
```

```
si3 0.18750
```

```
sp3 -21 0
```

```
# SI4 SP4
```

```
L D
```

```
7.173 0.0035
```

```
8.088 0.0085
```

```
8.146 0.076
```

```
8.428 0.00113
```

```
9.213 0.0102
```

```
9.316 0.00093
```

```
9.343 0.054
```

9.488	0.0148
9.646	0.0167
9.875	0.000303
10.895	0.01
11.130	0.000259
11.217	0.0032
11.277	0.0046
55.735	0.000131
56.280	0.187
57.535	0.326
64.948	0.0362
65.222	0.0698
65.652	0.00158
66.982	0.024
67.181	0.00372

c Materials

m1	1000.04p	0.6667	8000.04p	0.3333
m2	13000.04p	1		
m3	74000.04p			
c /				
nps	50000000			